Metamaterials for Manipulating Thermal Radiation: Transparency, Cloak, and Expander

Liujun Xu and Jiping Huang*

Department of Physics, State Key Laboratory of Surface Physics, and Key Laboratory of Micro and Nano Photonic Structures (MOE), Fudan University, 200438 Shanghai, China

(Received 9 August 2019; revised manuscript received 21 September 2019; published 22 October 2019)

Existing thermal metamaterials are mostly designed to work at room temperature, where thermal conduction is the dominant method of heat transfer. Unfortunately, as the temperature increases, thermal radiation becomes non-negligible, and hence these thermal metamaterials can no longer work. The inability to handle thermal radiation largely limits practical applications at high temperatures, such as thermal protection. To solve this problem, here we propose an effective-medium theory to manipulate thermal radiation with the Rosseland diffusion approximation. This theory helps to design three radiative metamaterials even with anisotropic geometries, including transparency, cloak, and expander. Theoretical analyses are further confirmed by finite-element simulations, which indicate that these radiative metamaterials behave well in both steady and transient states. This work not only offers an effective-medium theory to manipulate thermal radiation but also designs three radiative metamaterials. These results may provide hints for novel thermal management and have potential applications in radiative camouflage, radiative diodes, etc.

DOI: 10.1103/PhysRevApplied.12.044048

I. INTRODUCTION

Since the proposal of transformation thermotics [1,2], thermal metamaterials have experienced great developments and abundant achievements have been made. The capability of thermal management is largely improved with thermal metamaterials, such as thermal transparency [3–6], thermal cloak [7–12], thermal expander [13], etc. For thermal transparency the aim is to design a shell according to the inside core and ensure the temperature field outside the shell is undistorted. A thermal cloak can protect any object inside it from being detected, which can be realized by setting the core in a transparency scheme to be insulated. A thermal expander can efficiently enlarge a small source into a large one, which is based on two thermal cloaks. Moreover, thermal convection has also attracted much attention [14–16]. These thermal metamaterials provide powerful approaches to thermal management.

Unfortunately, none of these thermal metamaterials can work at high temperatures, where thermal radiation becomes the dominant method of heat transfer. Thermal radiation is of great significance, and has attracted much research interest, such as radiative cooling [17–19] and thermal memory [20,21]. However, metamaterials designed for manipulating thermal radiation have rarely been studied due to the lack of appropriate theories. In consideration of practical applications such as thermal protection at high temperatures, a theory to manipulate thermal radiation efficiently is urgently needed.

Here we propose an effective-medium theory to design radiative metamaterials with the Rosseland diffusive approximation. By designing the related parameters (mainly thermal conductivity and the Rosseland mean extinction coefficient) of a core-shell structure, we realize three radiative metamaterials even with anisotropic geometries, including transparency, cloak, and expander; see Figs. 1(a)–1(c). Finite-element simulations further confirm our theoretical analyses, which indicate that these radiative metamaterials are well behaved in both steady and transient states. We begin by presenting the theory.

II. THEORY

We consider a passive and steady process of heat transfer, where the total heat flux $\mathbf{J}_{\text{total}}$ (composed of the conductive flux $\mathbf{J}_{\text{con}}$ and the radiative flux $\mathbf{J}_{\text{rad}}$) is divergency-free:

$$\nabla \cdot \mathbf{J}_{\text{total}} = \nabla \cdot (\mathbf{J}_{\text{con}} + \mathbf{J}_{\text{rad}}) = 0. \tag{1}$$

The conductive flux $\mathbf{J}_{\text{con}}$ is dominated by the Fourier law:

$$\mathbf{J}_{\text{con}} = -\kappa \nabla T, \tag{2}$$

where κ is the thermal conductivity. The radiative flux $\mathbf{J}_{\text{rad}}$ is given by the Rosseland diffusion approximation:

$$\mathbf{J}_{\text{rad}} = -\gamma T^3 \nabla T, \tag{3}$$

*jphuang@fudan.edu.cn

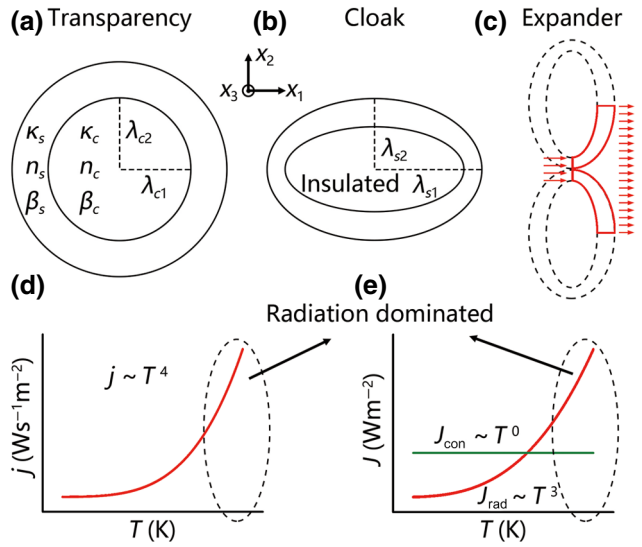

FIG. 1. (a) Thermal transparency, (b) thermal cloak, and (c) thermal expander. (d),(e) Radiative emittance j, conductive flux $\mathbf{J}_{\rm con}$, and radiative flux $\mathbf{J}_{\rm rad}$ as a function of temperature T.

where $\gamma = 16\beta^{-1}n^2\sigma/3$ can be regarded as the radiative coefficient, where β is the Rosseland mean extinction coefficient, n is the relative refractive index, and σ is the Stefan-Boltzmann constant $\left(5.67 \times 10^{-8}\ \mathrm{W\,m^{-2}\,K^{-4}}\right)$.

We consider a three-dimensional core-shell structure [Fig. 1(a)] that has a core with thermal conductivity κ_c, Rosseland mean extinction coefficient β_c, and relative refractive index n_c (radiative coefficient γ_c) coated by a shell with corresponding parameters κ_s, β_s, and n_s (radiative coefficient γ_s). The subscript c (s) denotes the core (shell) throughout this work. The semiaxis lengths of the core and shell are λ_{ci} and λ_{si} $(i = 1, 2, 3)$, respectively. We suppose that the ratio γ/κ of the core-shell structure is a constant α, say, $\gamma_c/\kappa_c = \gamma_s/\kappa_s = \alpha$. The physical intension is to realize the same effect of conduction and radiation. Then, Eq. (1) can be rewritten as

$$\begin{aligned}\nabla\cdot\left(-\kappa\nabla T-\alpha\kappa T^3\nabla T\right) &= \nabla\cdot\left[-\kappa\left(1+\alpha T^3\right)\nabla T\right]\\ &= \nabla\cdot\left[-\kappa\nabla\left(T+\alpha T^4/4\right)\right]=0.\end{aligned} \tag{4}$$

We perform a variable substitution $\varphi = T + \alpha T^4/4$, thus yielding

$$\nabla\cdot(-\kappa\nabla\varphi) = 0. \tag{5}$$

Therefore, we convert the formula with strong nonlinearity [Eq. (1)] into a linear one [Eq. (5)].

To proceed we introduce ellipsoidal coordinates (ρ, ξ, η)

$$\begin{aligned}&\frac{x^2}{\rho+\lambda_1^2}+\frac{y^2}{\rho+\lambda_2^2}+\frac{z^2}{\rho+\lambda_3^2}=1\ \text{(confocal ellipsoids)},\\ &\frac{x^2}{\xi+\lambda_1^2}+\frac{y^2}{\xi+\lambda_2^2}+\frac{z^2}{\xi+\lambda_3^2}=1\ \text{(hyperboloids of one sheet)},\\ &\frac{x^2}{\eta+\lambda_1^2}+\frac{y^2}{\eta+\lambda_2^2}+\frac{z^2}{\eta+\lambda_3^2}=1\ \text{(hyperboloids of two sheets)},\end{aligned} \tag{6}$$

where λ_1, λ_2, and λ_3 are three constants, satisfying $\rho > -\lambda_1^2 > \xi > -\lambda_2^2 > \eta > -\lambda_3^2$. Equation (5) can be expressed in ellipsoidal coordinates as

$$\frac{\partial}{\partial\rho}\left(g(\rho)\frac{\partial\varphi}{\partial\rho}\right)+\frac{g(\rho)}{\rho+\lambda_i^2}\frac{\partial\varphi}{\partial\rho}=0, \tag{7}$$

where $g(\rho)=\sqrt{\left(\rho+\lambda_1^2\right)\left(\rho+\lambda_2^2\right)\left(\rho+\lambda_3^2\right)}$. Equation (7) has a solution as

$$\varphi=\left(u+v\int_0^{\rho}\left(\rho+\lambda_i^2\right)^{-1}g(\rho)^{-1}\,d\rho\right)x_i, \tag{8}$$

where u and v are two constants, and x_i $(i = 1, 2, 3)$ denotes Cartesian coordinates. We define the temperatures (after variable substitution) of the core, shell, and background as φ_c, φ_s, and φ_b, respectively. They can be expressed as

$$\begin{aligned}\varphi_c &= u_c x_i,\\ \varphi_s &= \left(u_s+v_s\int_{\rho_c}^{\rho}\left(\rho+\lambda_i^2\right)^{-1}g(\rho)^{-1}\,d\rho\right)x_i,\\ \varphi_b &= u_b x_i,\end{aligned} \tag{9}$$

where u_c, u_s, and v_s can be determined by boundary conditions. The exterior surfaces of the core and shell are denoted by ρ_c and ρ_s, where boundary conditions are given by continuities of temperatures and normal heat fluxes, thus yielding

$$\begin{aligned}u_c &= u_s,\\ u_b &= u_s+v_s\int_{\rho_c}^{\rho_s}\left(\rho+\lambda_i^2\right)^{-1}g(\rho)^{-1}\,d\rho,\\ u_c &= 2v_s\kappa_s\left(\kappa_c-\kappa_s\right)^{-1}g(\rho_c)^{-1},\\ u_b &= 2v_s\kappa_s\left(\kappa_{ei}-\kappa_s\right)^{-1}g(\rho_s)^{-1},\end{aligned} \tag{10}$$

where κ_{ei} is the effective thermal conductivity of the core-shell structure along the direction of x_i. Solving Eq. (10) can directly give the expression for κ_{ei}. Nevertheless, it is a

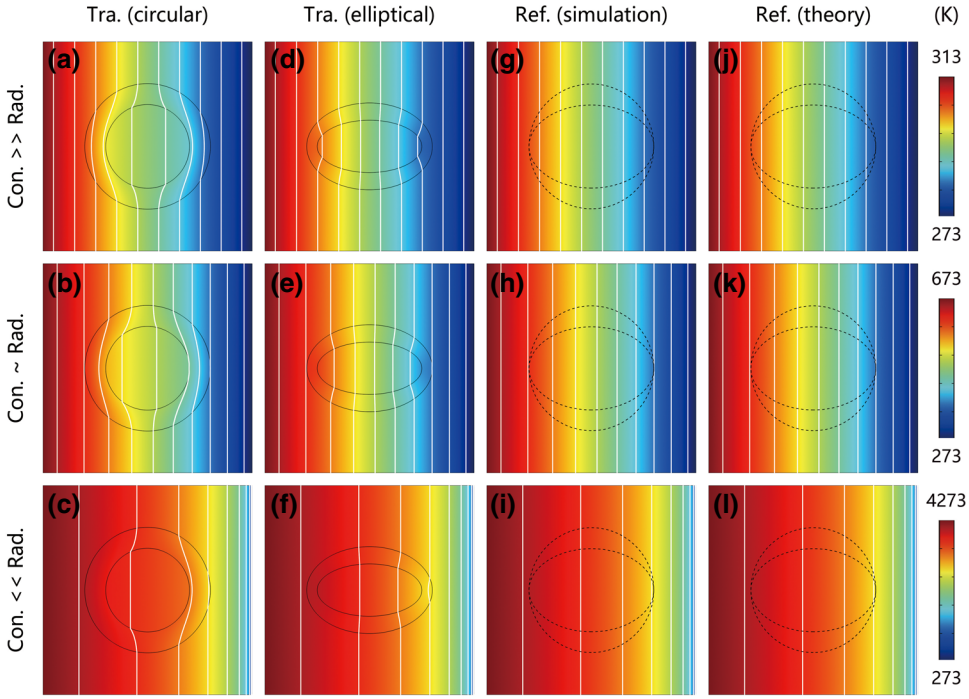

FIG. 2. Steady-state results for thermal transparency. (a)–(c) $\lambda_{c1} = \lambda_{c2} = 2$ cm, $\lambda_{s1} = \lambda_{s2} = 3$ cm, $\kappa_c = 2$ W m^{-1} K^{-1}, $\beta_c = 50$ m^{-1}, $\kappa_s = 0.62$ W m^{-1} K^{-1}, and $\beta_s = 161.1$ m^{-1}. (d)–(f) $\lambda_{c1} = 2.5$ cm, $\lambda_{c2} = 1.25$ cm, $\lambda_{s1} = 3$ cm, $\lambda_{s2} = 2.08$ cm, $\kappa_c = 0.5$ W m^{-1} K^{-1}, $\beta_c = 200$ m^{-1}, $\kappa_s = 1.61$ W m^{-1} K^{-1}, and $\beta_s = 62$ m^{-1}. (g)–(i) References with pure background parameters. (j)–(l) Theoretical temperature distributions of the references. Circular (elliptical) dashed lines are plotted for comparison with circular (elliptical) transparency. Con., conduction; Rad., radiation; Ref., reference; Tra., transparency.

complex formula that requires simplification. For this purpose, we define the semiaxis lengths of the core λ_{ci} and shell λ_{si} as

$$\begin{aligned} \lambda_{ci} &= \sqrt{\lambda_i^2 + \rho_c}, \\ \lambda_{si} &= \sqrt{\lambda_i^2 + \rho_s}, \end{aligned} \tag{11}$$

where $i = 1, 2, 3$. Thus, the volume fraction f can be expressed as

$$f = \lambda_{c1}\lambda_{c2}\lambda_{c3} / (\lambda_{s1}\lambda_{s2}\lambda_{s3}) = g(\rho_c) / g(\rho_s). \tag{12}$$

We also define the shape factor d_{wi} along the direction of x_i as

$$\begin{aligned} d_{wi} = \frac{\lambda_{w1}\lambda_{w2}\lambda_{w3}}{2} \int_0^\infty \left(\tau + \lambda_{wi}^2\right)^{-1} \\ \times \left[\left(\tau + \lambda_{w1}^2\right)\left(\tau + \lambda_{w2}^2\right)\left(\tau + \lambda_{w3}^2\right)\right]^{-1/2} d\tau, \end{aligned} \tag{13}$$

where the subscript w can take c or s, representing the shape factor of the core or shell. Thus, we can derive

$$\begin{aligned} &\int_{\rho_c}^{\rho_s} \left(\rho + \lambda_i^2\right)^{-1} g(\rho)^{-1} d\rho \\ &= \int_{\rho_c}^{\infty} \left(\rho + \lambda_i^2\right)^{-1} g(\rho)^{-1} d\rho \\ &- \int_{\rho_s}^{\infty} \left(\rho + \lambda_i^2\right)^{-1} g(\rho)^{-1} d\rho \\ &= 2d_{ci} g(\rho_c)^{-1} - 2d_{si} g(\rho_s)^{-1}. \end{aligned} \tag{14}$$

Finally, we can derive a brief expression for κ_{ei} as

$$\kappa_{ei} = \kappa_s \left(\frac{f(\kappa_c - \kappa_s)}{\kappa_s + (d_{ci} - f d_{si})(\kappa_c - \kappa_s)} + 1 \right). \tag{15}$$

This is a standard method to calculate the Laplace equation [22]. The shape factors satisfy the sum rule $d_{w1} + d_{w2} + d_{w3} = 1$. The effective thermal conductivity of any core-shell structure can, in principle, be derived with Eq. (15). However, only when the core-shell structure is confocal or concentric can Eq. (15) predict the effective thermal conductivity strictly. Moreover, Eq. (15) can also be reduced to handle cylindrical (two-dimensional) cases by taking $\lambda_{w3} = \infty$, thus yielding $d_{w1} = \lambda_{w2} / (\lambda_{w1} + \lambda_{w2})$, $d_{w2} = \lambda_{w1} / (\lambda_{w1} + \lambda_{w2})$, and $d_{w3} = 0$ ($d_{w1} + d_{w2} + d_{w3} = 1$ is still satisfied).

Since we have supposed that γ/κ is a constant, the effective radiative coefficient can be directly written as

$$\gamma_{ei} = \gamma_s \left(\frac{f(\gamma_c - \gamma_s)}{\gamma_s + (d_{ci} - f d_{si})(\gamma_c - \gamma_s)} + 1 \right), \tag{16}$$

where γ_{ei} is the effective radiative coefficient of the core-shell structure along the direction of x_i. Equations (15) and (16) can predict the effective thermal conductivity and effective radiative coefficient. The only requirement is to keep γ/κ constant to realize the same effect of conduction and radiation.

III. FINITE-ELEMENT SIMULATIONS

We perform finite-element simulations with COMSOL MULTIPHYSICS [23] to validate the theoretical analyses.

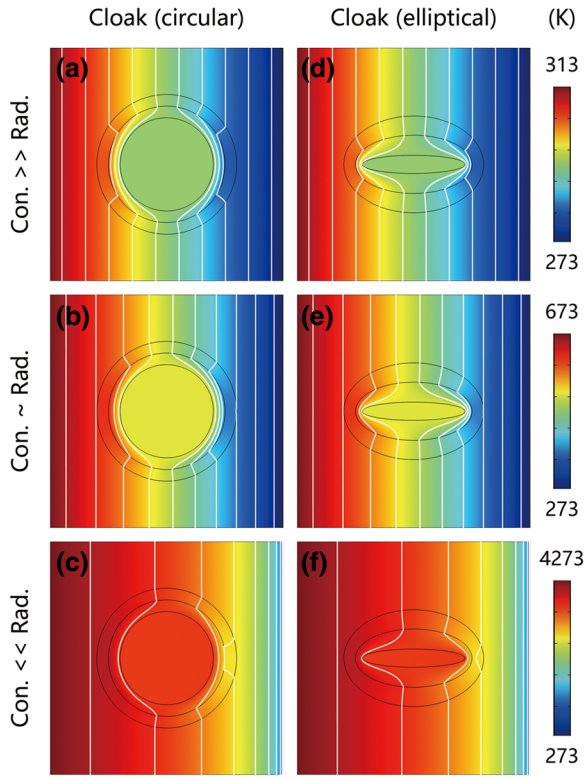

FIG. 3. Steady-state simulations of the thermal cloak. An inner object is coated by an insulated layer with $\kappa = 10^{-5}$ W m^{-1} K^{-1} and $\beta = 10^{5}$ m^{-1}. Since the heat flux cannot enter the insulated layer, the inner object plus the insulated layer can be equivalently regarded as an insulated core with $\kappa_c = 10^{-5}$ W m^{-1} K^{-1} and $\beta_c = 10^{5}$ m^{-1}. Other parameters are as follows: (a)–(c) $\lambda_{c1} = \lambda_{c2} = 2.5$ cm, $\lambda_{s1} = \lambda_{s2} = 3$ cm, $\kappa_s = 5.54$ W m^{-1} K^{-1}, and $\beta_s = 18.1$ m^{-1}; (d)–(f) $\lambda_{c1} = 2.5$ cm, $\lambda_{c2} = 1.25$ cm, $\lambda_{s1} = 3$ cm, $\lambda_{s2} = 2.08$ cm, $\kappa_s = 2.35$ W m^{-1} K^{-1}, and $\beta_s = 42.5$ m^{-1}. Con., conduction; Rad., radiation.

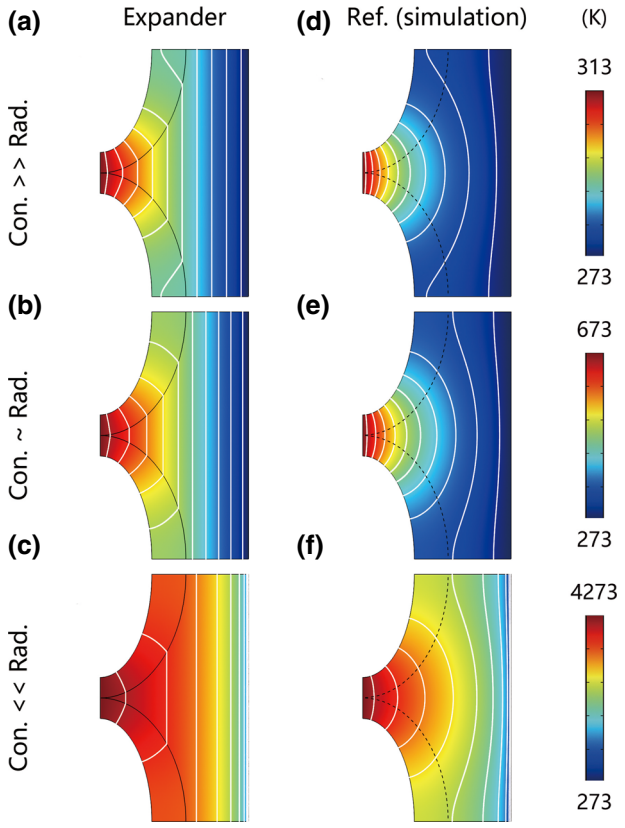

FIG. 4. Steady-state simulations of the thermal expander. The sizes are $\lambda_{c1} = 2.08$ cm, $\lambda_{c2} = 4.17$ cm, $\lambda_{s1} = 3.46$ cm, and $\lambda_{s2} = 5$ cm, and the width between hot and cold sources is 6 cm. Other parameters are as follows: (a)–(c) $\kappa_s = 4.91$ W m^{-1} K^{-1} and $\beta_s = 20.3$ m^{-1}; (d)–(f) pure background parameters. Con., conduction; Rad., radiation.

Without loss of generality, we consider a two-dimensional case with size 10×10 cm^2, and directly use the template of "Heat Transfer with Radiation in Participating Media." Then, we input the relative refractive index of all regions as 1, and set the thermal conductivity and the Rosseland mean extinction coefficient of the background to 1 W m^{-1} K^{-1} and 100 m^{-1}, respectively. These values are close to those of practical materials such as organic glass, which meet the requirements of the Rosseland diffusion approximation.

The Stefan-Boltzmann law suggests that the radiative emittance j is proportional to T^4, as qualitatively shown in Fig. 1(d). In the presence of the same temperature gradient, the conductive flux $\mathbf{J}_{\rm con}$ is independent of concrete temperatures, whereas the radiative flux $\mathbf{J}_{\rm rad}$ is proportional to T^3, as qualitatively presented in Fig. 1(e). These qualitative analyses indicate that thermal radiation is of great significance at high temperatures. Thus, three temperature intervals are applied in our finite-element simulations: (i) 273–313 K, indicating a small upper temperature limit where conduction is dominant; (ii) 273–673 K, indicating a medium upper temperature limit where conduction and radiation are roughly equal; (iii) 273–4273 K, indicating a large upper temperature limit where radiation is dominant.

For thermal transparency the aim is to design a shell according to the object, ensuring the temperature profile outside the shell is undistorted; see Fig. 2. When the parameters are delicately designed according to Eqs. (15) and (16), the temperature profile outside the shell is undistorted [Figs. 2(a)–2(c) or Figs. 2(d)–2(f)] as if there were not a core-shell structure in the center [Figs. 2(g)–2(i)]. Figures 2(j)–2(l) demonstrate the theoretical results for the references with the same parameters as for Figs. 2(g)–2(i). The temperature distributions can be calculated as follows. We denote the temperatures of the left and right boundaries as T_l and T_r, thus yielding $\varphi_l = T_l + \alpha T_l^4/4$ and $\varphi_r = T_r + \alpha T_r^4/4$, respectively. According to Eq. (5), the temperature distribution for a reference case takes the form $\varphi = (\varphi_r - \varphi_l)\, x_1/b + (\varphi_r + \varphi_l)\,/2$, where b is the length between the left boundary and the right boundary.

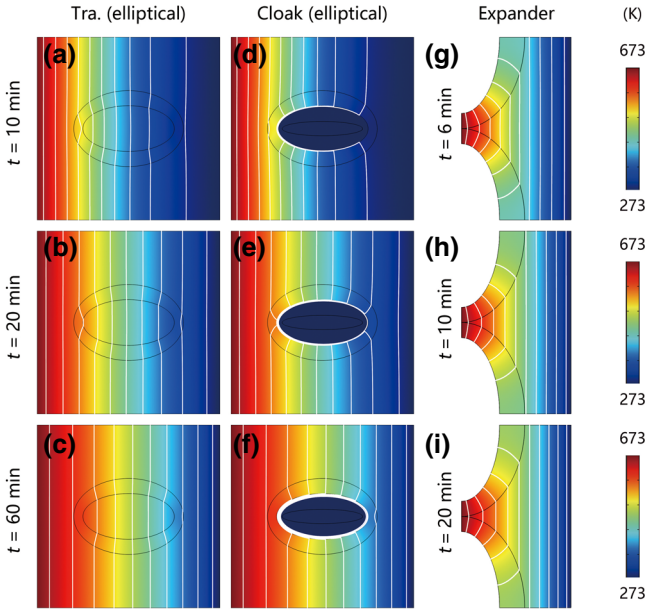

FIG. 5. Transient simulations of transparency, cloak, and expander. The sizes and material parameters for (a)–(c), (d)–(f), and (g)–(i) are the same as those for Figs. 2(d)–2(f), Figs. 3(d)–3(f), and Figs. 4(a)–4(c), respectively. The product of the density and heat capacity of the background is $\rho C = 10^6\ \mathrm{J\,m^{-3}\,K^{-1}}$. Other parameters are as follows: (a)–(c) $(\rho C)_c = 5 \times 10^5\ \mathrm{J\,m^{-3}\,K^{-1}}$ and $(\rho C)_s = 1.61 \times 10^6\ \mathrm{Jm^{-3}\,K^{-1}}$; (d)–(f) $(\rho C)_s = 2.35 \times 10^6\ \mathrm{J\,m^{-3}\,K^{-1}}$; (g)–(i) $(\rho C)_s = 5 \times 10^5\ \mathrm{J\,m^{-3}\,K^{-1}}$. Tra., transparency.

By solving $\varphi = T + \alpha T^4/4$, we can numerically derive the temperature distributions with respect to T. The same temperature profiles for the references (simulation and theory) indicate validation of the theoretical analyses. Moreover, with a small upper temperature limit where conduction is dominant, the temperature gradient outside the shell is almost uniform; see Figs. 2(a), 2(d), 2(g), and 2(j). As the upper temperature limit increases, radiation starts exerting an influence, thus yielding nonuniform temperature gradients outside the shell; see Figs. 2(b), 2(e), 2(h), 2(k), 2(c), 2(f), 2(i), and 2(l).

A thermal cloak can protect any object inside it from being detected, and its parameters are independent of the object. For this purpose, an insulated layer is required to keep the heat flux off the object. Then, the object plus the insulated layer can be equivalently regarded as an insulated core, say, $\kappa_c = \gamma = 0$. Furthermore, we design a shell according to Eqs. (15) and (16) to remove the effect of the insulated core. The simulation results are presented in Fig. 3. Clearly, the isotherms are kept off the object, indicating that the heat flux cannot enter the object. Meanwhile, the temperature profiles of the background are not distorted, thus yielding the cloaking effect.

A thermal expander can efficiently enlarge a small source into a large one on the basis of the design of two elliptical cloaks. Concretely speaking, we put two elliptical cloaks together, and take out a quarter of the whole structure as an expander; see Fig. 1(c). As ensured by the uniqueness theorem in thermotics [24], the temperature distribution of the background is not distorted, thus yielding the expander effect. Finite-element simulations are presented in Figs. 4(a)–4(c). Clearly, the isotherms of the background are straight, indicating the excellent performance. However, a pure background material strongly distorts the isotherms of the background; see Figs. 4(d)–4(f). This device is flexible to adjust the source sizes and has applications in uniform heating and effective dissipation.

The above results consider only the steady states. These radiative metamaterials can also be extended to transient states if we consider density and heat capacity. To design transient transparency and a transient cloak, we set the heat diffusivity $\kappa/(\rho C)$ to be a constant. Although this is an approximate method, its performance is still satisfactory. The corresponding results at $t = 10$, 20, and 60 min are presented in Figs. 5(a)–5(c) and Figs. 5(d)–5(f), respectively. To design a transient expander, we use the optimization method and set the diffusivity of the shell larger than that of the background to achieve the best transient effect. The corresponding results at $t = 6$, 10, and 20 min are presented in Figs. 5(g)–5(i).

IV. DISCUSSION AND CONCLUSION

We give the theoretical designs of three radiative metamaterials based on the effective-medium theory for thermal radiation. For experimental demonstrations, we can fabricate two-dimensional samples whose surfaces are covered by insulated films to confine thermal radiation in two dimensions. The background material chosen in this work is similar to organic glass, and aerogel is an excellent candidate for the insulated material when designing a thermal cloak. Moreover, the present theory is also promising to extend those novel conductive metamaterials with layered structures (such as thermal bending) [25–31] to the radiative regimes. Although the effective-medium theory is powerful, it cannot strictly handle core-shell problems with complex shapes.

The validity of this work is based on the Fourier law and the Rosseland diffusion approximation. Thermal conduction is handled with the Fourier law [Eq. (2)], which is an appropriate hypothesis at the macroscale. However, at the nanoscale, if the phonon effect is taken into consideration [32–36], the Fourier law may be invalid. Meanwhile, thermal radiation under our consideration is handled with the Rosseland diffusion approximation [Eq. (3)], which requires the participating media to be optically thick. That is, photons of thermal radiation propagate only a short distance before being absorbed or scattered. Many other radiative models, such as those considering near-field effects [37–40], remain to be further explored.

To sum up, we propose an effective-medium theory to manipulate thermal radiation and design three radiative metamaterials, including transparency, cloak, and expander. All theoretical analyses are confirmed by finite-element simulations. These radiative metamaterials are well behaved in both steady and transient states. Certainly, they have potential applications in designing thermal camouflage [41–45] and thermal diodes [32,46] in the regimes at high temperatures where thermal radiation is the dominant effect.

ACKNOWLEDGMENTS

We are grateful to Gaole Dai for beneficial discussions. We acknowledge financial support by the National Natural Science Foundation of China under Grant No. 11725521.

[1] C. Z. Fan, Y. Gao, and J. P. Huang, Shaped graded materials with an apparent negative thermal conductivity, Appl. Phys. Lett. **92**, 251907 (2008).
[2] T. Y. Chen, C. N. Weng, and J. S. Chen, Cloak for curvilinearly anisotropic media in conduction, Appl. Phys. Lett. **93**, 114103 (2008).
[3] X. He and L. Z. Wu, Thermal transparency with the concept of neutral inclusion, Phys. Rev. E **88**, 033201 (2013).
[4] L. W. Zeng and R. X. Song, Experimental observation of heat transparency, Appl. Phys. Lett. **104**, 201905 (2014).
[5] T. Z. Yang, X. Bai, D. L. Gao, L. Z. Wu, B. W. Li, J. T. L. Thong, and C. W. Qiu, Invisible sensors: Simultaneous sensing and camouflaging in multiphysical fields, Adv. Mater. **27**, 7752 (2015).
[6] L. J. Xu, S. Yang, and J. P. Huang, Thermal Transparency Induced by Periodic Interparticle Interaction, Phys. Rev. Appl. **11**, 034056 (2019).
[7] S. Narayana and Y. Sato, Heat Flux Manipulation with Engineered Thermal Materials, Phys. Rev. Lett. **108**, 214303 (2012).
[8] H. Y. Xu, X. H. Shi, F. Gao, H. D. Sun, and B. L. Zhang, Ultrathin Three-dimensional Thermal Cloak, Phys. Rev. Lett. **112**, 054301 (2014).
[9] T. C. Han, X. Bai, D. L. Gao, J. T. L. Thong, B. W. Li, and C. W. Qiu, Experimental Demonstration of a Bilayer Thermal Cloak, Phys. Rev. Lett. **112**, 054302 (2014).
[10] Y. G. Ma, Y. C. Liu, M. Raza, Y. D. Wang, and S. L. He, Experimental Demonstration of a Multiphysics Cloak: Manipulating Heat Flux and Electric Current Simultaneously, Phys. Rev. Lett. **113**, 205501 (2014).
[11] T. C. Han, X. Bai, J. T. L. Thong, B. W. Li, and C. W. Qiu, Full control and manipulation of heat signatures: Cloaking, camouflage and thermal metamaterials, Adv. Mater. **26**, 1731 (2014).
[12] Y. Li, K. J. Zhu, Y. G. Peng, W. Li, T. Z. Yang, H. X. Xu, H. Chen, X. F. Zhu, S. H. Fan, and C. W. Qiu, Thermal meta-device in analogue of zero-index photonics, Nat. Mater. **18**, 48 (2018).
[13] T. C. Han, P. Yang, Y. Li, D. Y. Lei, B. W. Li, K. Hippalgaonkar, and C. W. Qiu, Full-parameter omnidirectional thermal metadevices of anisotropic geometry, Adv. Mater. **30**, 1804019 (2018).
[14] G. L. Dai, J. Shang, and J. P. Huang, Theory of transformation thermal convection for creeping flow in porous media: Cloaking, concentrating, and camouflage, Phys. Rev. E **97**, 022129 (2018).
[15] G. L. Dai and J. P. Huang, A transient regime for transforming thermal convection: Cloaking, concentrating and rotating creeping flow and heat flux, J. Appl. Phys. **124**, 235103 (2018).
[16] Y. Li, Y. G. Peng, L. Han, M. A. Miri, W. Li, M. Xiao, X. F. Zhu, J. L. Zhao, A. Alu, S. H. Fan, and C. W. Qiu, Anti-parity-time symmetry in diffusive systems, Science **364**, 170 (2019).
[17] A. P. Raman, M. A. Anoma, L. X. Zhu, E. Rephaeli, and S. H. Fan, Passive radiative cooling below ambient air temperature under direct sunlight, Nature **515**, 540 (2014).
[18] Y. Zhai, Y. G. Ma, S. N. David, D. L. Zhao, R. N. Lou, G. Tan, R. G. Yang, and X. B. Yin, Scalable-manufactured randomized glass-polymer hybrid metamaterial for daytime radiative cooling, Science **355**, 1062 (2017).
[19] Z. Chen, L. X. Zhu, W. Li, and S. H. Fan, Simultaneously and synergistically harvest energy from the sun and outer space, Joule **3**, 101 (2018).
[20] V. Kubytskyi, S. A. Biehs, and P. Ben-Abdallah, Radiative Bistability and Thermal Memory, Phys. Rev. Lett. **113**, 074301 (2014).
[21] J. Ordonez-Miranda, Y. Ezzahri, J. A. Tiburcio-Moreno, K. Joulain, and J. Drevillon, Radiative Thermal Memristor, Phys. Rev. Lett. **123**, 025901 (2019).
[22] G. W. Milton, *The Theory of Composites* (Cambridge University Press, Cambridge, 2004), Vol. 124.
[23] http://www.comsol.com/.
[24] L. J. Xu, R. Z. Wang, and J. P. Huang, Camouflage thermotics: A cavity without disturbing heat signatures outside, J. Appl. Phys. **123**, 245111 (2018).
[25] K. P. Vemuri and P. R. Bandaru, Anomalous refraction of heat flux in thermal meta-materials, Appl. Phys. Lett. **104**, 083901 (2014).
[26] T. Z. Yang, K. P. Vemuri, and P. R. Bandaru, Experimental evidence for the bending of heat flux in a thermal metamaterial, Appl. Phys. Lett. **105**, 083908 (2014).
[27] K. P. Vemuri, F. M. Canbazoglu, and P. R. Bandaru, Guiding conductive heat flux through thermal metamaterials, Appl. Phys. Lett. **105**, 193904 (2014).
[28] R. S. Kapadia and P. R. Bandaru, Heat flux concentration through polymeric thermal lenses, Appl. Phys. Lett. **105**, 233903 (2014).
[29] L. J. Xu, S. Yang, and J. P. Huang, Thermal theory for heterogeneously architected structure: Fundamentals and application, Phys. Rev. E **98**, 052128 (2018).
[30] L. J. Xu, S. Yang, and J. P. Huang, Designing effective thermal conductivity of materials of core-shell structure: Theory and simulation, Phys. Rev. E **99**, 022107 (2019).
[31] L. J. Xu, S. Yang, and J. P. Huang, Passive Metashells with Adaptive Thermal Conductivities: Chameleonlike Behavior and its Origin, Phys. Rev. Appl. **11**, 054071 (2019).
[32] B. W. Li, L. Wang, and G. Casati, Thermal Diode: Rectification of Heat Flux, Phys. Rev. Lett. **93**, 184301 (2004).

[33] B. W. Li, L. Wang, and G. Casati, Negative differential thermal resistance and thermal transistor, Appl. Phys. Lett. **88**, 143501 (2006).

[34] L. Wang and B. W. Li, Thermal Logic Gates: Computation with Phonons, Phys. Rev. Lett. **99**, 177208 (2007).

[35] N. B. Li, J. Ren, L. Wang, G. Zhang, P. Hanggi, and B. W. Li, Phononics: Manipulating heat flow with electronic analogs and beyond, Rev. Mod. Phys. **84**, 1045 (2012).

[36] H. Bao, J. Chen, X. K. Gu, and B. Y. Cao, A review of simulation methods in micro/nanoscale heat conduction, ES Energy Environ. **1**, 16 (2018).

[37] P. Ben-Abdallah and S. A. Biehs, Near-field Thermal Transistor, Phys. Rev. Lett. **112**, 044301 (2014).

[38] V. Fernandez-Hurtado, F. J. Garcia-Vidal, S. F. Fan, and J. C. Cuevas, Enhancing Near-field Radiative Heat Transfer with Si-based Metasurfaces, Phys. Rev. Lett. **118**, 203901 (2017).

[39] M. Ghashami, H. Y. Geng, T. Kim, N. Iacopino, S. K. Cho, and K. Park, Precision Measurement of Phonon-polaritonic Near-field Energy Transfer Between Macroscale Planar Structures Under Large Thermal Gradients, Phys. Rev. Lett. **120**, 175901 (2018).

[40] G. T. Papadakis, B. Zhao, S. Buddhiraju, and S. H. Fan, Gate-tunable near-field heat transfer, ACS Photonics **6**, 709 (2019).

[41] R. Hu, S. L. Zhou, Y. Li, D. Y. Lei, X. B. Luo, and C. W. Qiu, Illusion thermotics, Adv. Mater. **30**, 1707237 (2018).

[42] Y. R. Qu, Q. Li, L. Cai, M. Y. Pan, P. Ghosh, K. K. Du, and M. Qiu, Thermal camouflage based on the phasechanging material GST, Light-Sci. Appl. **7**, 26 (2018).

[43] Y. Li, X. Bai, T. Z. Yang, H. Luo, and C. W. Qiu, Structured thermal surface for radiative camouflage, Nat. Commun. **9**, 273 (2018).

[44] R. Hu, S. Y. Huang, M. Wang, X. L. Luo, J. Shiomi, and C. W. Qiu, Encrypted thermal printing with regionalization transformation, Adv. Mater. **31**, 1807849 (2019).

[45] J. X. Li, Y. Li, T. L. Li, W. Y. Wang, L. Q. Li, and C. W. Qiu, Doublet Thermal Metadevice, Phys. Rev. Appl. **11**, 044021 (2019).

[46] Y. Li, X. Y. Shen, Z. H. Wu, J. Y. Huang, Y. X. Chen, Y. S. Ni, and J. P. Huang, Temperature-dependent Transformation Thermotics: From Switchable Thermal Cloaks to Macroscopic Thermal Diodes, Phys. Rev. Lett. **115**, 195503 (2015).